Chapter 1

Introduction

1.1 Overview

Controlling the bond-selective dissociation of a molecule ABC,

$$\mathrm{A} + \mathrm{BC} \xleftarrow{\text{Path 1}} \mathrm{ABC} \xrightarrow{\text{Path 2}} \mathrm{AB} + \mathrm{C}$$

has been a fundamental challenge in the field of reaction dynamics for many decades [1, 2]. To tackle this problem, one requires sufficient information about the energetics (ΔG, ΔH, etc.), the reaction rates ($k(T)$), and the dissociation mechanism [3]. With sufficient knowledge of the chemical system at hand, one can devise mechanisms to manipulate its intrinsic thermodynamics or kinetics and thereby steer the reaction in the desired manner. Before laser technology became widespread, this manipulation was often accomplished using temperature or pressure variation, or with the help of a catalyst [4]. Such approaches are macroscopic in scale; the conditions of the reaction chamber are changed, and the reactants respond accordingly. In the 1980s, however, lasers began being used to prepare the reactant in a specific energy state—typically vibrational or electronic state—before allowing the chemical species to react. States or vibrational modes involved in the reaction of interest were identified and then excited with a matching laser frequency. The first work along these lines was accordingly termed *mode-selective chemistry*, and notable experiments using this approach were carried out by Crim and [5, 6, 7] and Zare [8, 9], who primarily studied the reactivity of isotopically substituted water, HOD, with thermal H atoms. In these experiments, a Nd:YAG laser, capable of producing pulses on the nanosecond scale, was tuned to excite specific vibrational modes of HOD. Due to the distinct stretching frequencies of H–OD and HO–D, at 3800 cm^{-1} and 2800 cm^{-1}, respectively, the molecule is an ideal model

system for mode-selective chemistry since the stretching modes are nearly uncoupled. This quality implies that the vibrational excitation remains localized in the mode, and intramolecular vibrational redistribution (IVR) is minimal.

In many molecular systems, however, the coupling between vibrational modes is not negligible, and IVR quickly funnels the energy out of the target mode and into other (undesired) modes. In such systems, mode-selective chemistry is ineffective. Instead, "coherent control" methods were developed to control chemical reactions based on quantum interference effects [10]. In general, coherent control refers to the creation of a coherent superposition of energy-resolved eigenstates—or a non-stationary wave packet—using laser light. By manipulating the relative phases of these eigenstates with laser pulses, one can obtain either constructive or destructive interference patterns, and the motion of the wave packet can be controlled. Brumer and Shapiro showed theoretically that the simultaneous one- and three-photon excitation of CH_3I at 266 nm can lead to different yields of iodine upon photodissociation of CH_3I [10]. Coherent control theory was heavily motivated by advances in femtosecond (1 fs$= 10^{-15}$ s) laser technology, pioneered by Zewail and co-workers [3, 11]. Laser pulses with femtosecond resolution are short enough to follow nuclear motion—the breaking and forming of bonds—in "real time". Their duration also implies that femtosecond laser pulses contain a broad range of frequency components, according to Heisenberg's uncertainty principle. Several coherent control strategies based on the manipulation of these laser pulses have been designed.

Hallmark advancements in the field of coherent laser control include the "pump-dump" approach, suggested by Tannor, Kosloff, and Rice, which makes use of ultrashort laser pulses to "pump" a quantum mechanical system to a specific state; after a well-defined time, a second "dump" laser drives the system down to a target state [12, 13]. In analogy, a "pump-probe" scenario was introduced by Zewail [14]; here, the delay between the pump and probe pulses is varied to follow the wave packet dynamics in real time. However, for molecular systems with many degrees of freedom coupled together, designing an electric field to drive the system to a target state is quite challenging due to the complex nature of the Hamiltonian. To circumvent this obstacle in controlling molecular dynamics of large systems, Shi, Woody, and Rabitz developed "optimal control theory". This application relies on engineering control concepts to maximize a specific product yield by optimizing the tunable laser field [15, 16]. Judson and Rabitz then extended this approach to include an evolutionary algorithm that directly compares the product yield with the desired output, iteratively re-optimizes the electric field, and thus solves the Schrödinger equation "on the fly" [17, 18]. This method was successfully tested experimentally in several systems: the branching ratios of different photodissociation

channels of $CpFe(CO)_2Cl$ were optimized using a learning evolutionary algorithm [19]; selective dissociation was controlled in polyatomic organic molecules [20]; and energy-flow pathways in a light-harvesting complex were directed with a feedback-optimized loop [21]. As a result of the adaptive learning algorithm, the optimized electric field profile is often extremely intricate. For some systems, however, it is possible to decipher the optimized laser pulse to uncover the reaction dynamics driving the system [22].

1.2 Infrared laser-mediated photodissociation

In addition to the schemes mentioned above, other mechanisms have been suggested to control reaction dynamics, including infrared (IR) laser-mediated photodissociation. This mechanism proceeds in the following manner: an IR pulse transfers energy into a single vibrational mode, or into a superposition of vibrational states, depending on the duration and shape of the applied IR light. If the IR light corresponds to one wavelength, as in continuous wave (cw) lasers, a single eigenstate or an overtone of a particular stretching vibration is excited, as shown in the work of Imre and Zhang [23, 24] and Crim [5, 6, 25, 26]. After the IR pulse is applied, the vibrationally excited bond will dissociate if a photolysis pulse is fired. The advantage of this mechanism is that the IR light need not be specially shaped or particularly short. However, the excited vibrational eigenstate is delocalized, so only a small fraction of the total population is actually excited. To increase the efficiency of the vibrational excitation, Manz and coworkers extended this approach to use a series of short (sub-picosecond), intense (20 TW/cm^2) IR laser pulses, such that nearly 100% of the initial population is transferred to the target state [27, 28, 29]. By decreasing the frequency of the laser as a function of time—or chirping the IR laser—one can even generate pulses that allow vibrational ladder climbing [30].

As the IR pulse is made even shorter ($\sim$ 100 femtoseconds), it begins to spread in the frequency domain and no longer corresponds to one color. This range of IR frequencies in an ultrashort laser pulse excites a superposition of vibrational states, or a wave packet, as demonstrated by Henriksen [31]. In the IR (or visible) frequency ranges, such ultrashort pulses contain only a few cycles, so they are referred to as *few-cycle* pulses. These cycles can be tuned to drive the bond oscillation, similar to a linearly forced harmonic oscillator. Henriksen went on to show that following the ultrashort IR pulse, when either the position or momentum is optimal, an ultrashort ($\sim$5 fs) ultraviolet (UV) laser pulse can vertically excite the molecule to a dissociative state, and the pre-excited bond will proceed to break. This mechanism was applied to control the bond-selective dissociation of HOD [31] and isotopically substituted ozone, $^{16}O^{16}O^{18}O$ [32]. In this

thesis, we will be pursuing bond-selective dissociation using the method presented by Henriksen, namely using a combination of ultrashort, few-cycle IR and UV laser pulses. Let us now take a more detailed look at this mechanism, which is depicted schematically in Figure 1.1. The lower potential energy curve in Figure 1.1 represents a ground

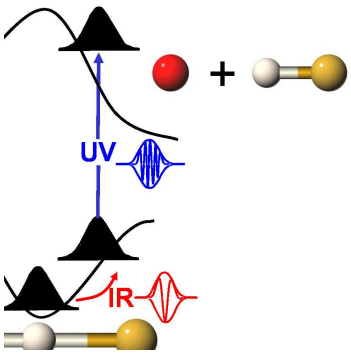

Figure 1.1: Selective bond breaking mediated by few-cycle IR + UV laser pulses. The IR pulse creates a wave packet whose motion corresponds to the extension and compression of the bonds. When the bond of interest has been maximally extended, the wave packet is located at the turning point of the oscillation. At this time, an ultrashort UV pulse is applied that excites the wave packet vertically to a bond-selective region of the upper state. The pre-excited bond proceeds to break, resulting in the formation of one set of products.

electronic state, and the upper curve could correspond to a higher-lying electronic state, or to an ionized (loss of an electron) state. A few-cycle IR pulse creates a wave packet that begins moving on the time scale corresponding to the period of the bond vibration. When the bond of interest has been maximally extended, the wave packet is located at the turning point of its oscillation (shown in Figure 1.1) and the momentum is nearly zero. At this time, the ultrashort UV pulse is applied. Alternatively, one could excite the wave packet at a time corresponding to maximum momentum to achieve selective bond-breaking [33]. The UV pulse is tuned to excite the wave packet vertically to the upper state. The duration of the UV pulse must be very short to take advantage of the optimal localization of the wave packet at the time of the vertical excitation. The pre-excited bond proceeds to break, resulting—ideally—in the exclusive formation of one set of products. In general, the mechanism benefits from short pulses since the wave packet initially created is compact, whereas over time, anharmonicity causes spreading and a loss of coherence in the wave packet. One drawback of using an IR pulse to excite a vibrational mode, or combination of modes, is that high intensities are often required to obtain detectable population transfer, even though intensities above 10 TW/cm^2 often lead to destructive processes or undesired ionization [30]. Therefore, unwanted molecular ionization can be a problematic competing process.

1.3 Control of molecular orientation

In the above-mentioned control scheme (*cf.* Figure 1.1), the molecules are assumed to have a fixed orientation with respect to the polarization of both the IR and UV laser fields. In other words, the molecules are oriented prior to the application of the few-cycle IR + UV laser pulses. Indeed, many simulated unimolecular dissociation reactions and bimolecular collision reactions are performed under the tacit assumption that the orientation of the reactants is known. For example, highly localized distributions of dissociation products have been reported for molecules that are optimally aligned or oriented in a laser field [34, 35]. Charron and coworkers demonstrated that the isotopes H^+ and D^+ can be separated along the laser polarization axis following the photodissociation of oriented HD^+ [35].

The assumption that reactants are oriented prior to any reaction is, however, the source of large discrepancy between theory and experiment. Quantifying molecular orientation becomes especially critical when one discusses collision probabilities, reaction yields, and the possible spatial separation of dissociation products. In fact, for randomly oriented molecules, laser control schemes often achieve only a low yield of bond-selective dissociation products [36]. The reason for this loss of effectiveness is two-fold. First, the molecule-field interaction is governed by the scalar product of the molecular dipole and the field vector; molecules that are aligned parallel to the electric field will experience a larger field strength than will those that lie perpendicular to the field. Thus, depending on the relative orientation of reactants in the laser field, the IR field can be more or less efficient at displacing the wave packet from its equilibrium position or momentum. Additionally, since the subsequent UV pulse is tuned to a specific vertical energy, it will only succeed at exciting those wave packets that have been pre-excited by the IR pulse to a specific region of the potential energy surface (PES). Therefore, the yield of dissociation products strongly depends on the initial orientation of reactants in the laser field. Controlling the molecular orientation should thus enhance the efficiency of both the IR and UV laser pulses in achieving bond-selective dissociation.

Along these lines, methods have been developed for aligning or orienting molecules prior to the control step. (For definitions of "alignment" and "orientation", see Section 2.5.3.) One "passive" approach involves using short IR laser pulses that will excite species of a particular orientation while leaving non-oriented molecules at rest [36, 37]. More common, however, are methods have been designed to achieve "active" alignment or orientation of molecules prior to the control step [38, 39, 40].

Experimental approaches to controlling molecular orientation include: the brute

force method in which a direct current (dc) electric field is applied [41, 42]; the scheme of coherent two-color laser excitation [43]; or the technique of hexapole state selection [44, 45]. Theoretically, Friedrich and Herschbach examined the possibility of exploiting rotational cooling that occurs in supersonic molecular beams to orient diatomic, linear or asymmetric top molecules. They coined the term "pendular states," or states which arise from an adiabatic interaction with the laser field, in which the molecule is confined to librate over a limited angular range [38]. They also showed that the orientation of polar molecules can be enhanced by a combined static field and pulsed nonresonant laser field [46], an approach that was successfully implemented by Sakai *et al.* for the triatomic OCS [47]. Henriksen modelled short, off-resonant plane polarized laser fields to control the orientation of a linear rigid rotor [48]. Dion *et al.* numerically demonstrated the orientation of HCN for two-frequency IR laser pulses [49].

Closely related to these studies, the problem of molecular alignment has also been treated extensively, both theoretically as well as experimentally. General theory on rotational excitation, molecular alignment, and rotational revivals, in both the adiabatic and nonadiabatic regimes, has received much attention from Seideman [50, 51, 52, 53]. Larsen and Stapelfeldt have aligned molecules such as I_2, ICl, CS_2, and CH_3I using an intense, nonresonant linearly polarized laser field, by taking advantage of molecular polarizability [54]. Stapelfeldt and Seideman have also addressed the challenge—experimentally and theoretically, respectively— of three-dimensional alignment by proposing the use of elliptically polarized laser fields [55, 56].

One of the more recent approaches to controlling molecular orientation involves using a half-cycle pulse (HCP), depicted schematically in Figure 1.2. Although this technique has of yet only been studied numerically [57, 58, 59], high-power (0.8 μJ) 500 fs HCPs in the THz (far-IR) range have been available for over ten years and are suitable for non-linear optics and multiphoton spectroscopy experiments [60]. In fact, numerical optimal control schemes that produce laser fields based on genetic algorithms have indicated that HCPs are the most effective in achieving a high degree of orientation [59, 61]. In this work, we will examine the ability of HCPs to orient molecules *prior* to applying few-cycle IR and UV pulses. Furthermore, we will see that molecular orientation is preserved over several picoseconds. Due to the revival behavior of rotational wave packets, recurrences of orientation are observed periodically, even under field-free conditions. On the time scale of rotational motion—*i.e.* picoseconds—vibrational motion can then be controlled using ultrashort ($5-50$ fs) laser pulses. Having reviewed the control mechanisms we will be using in our quantum dynamical simulations, we now turn our attention to triatomic model systems.

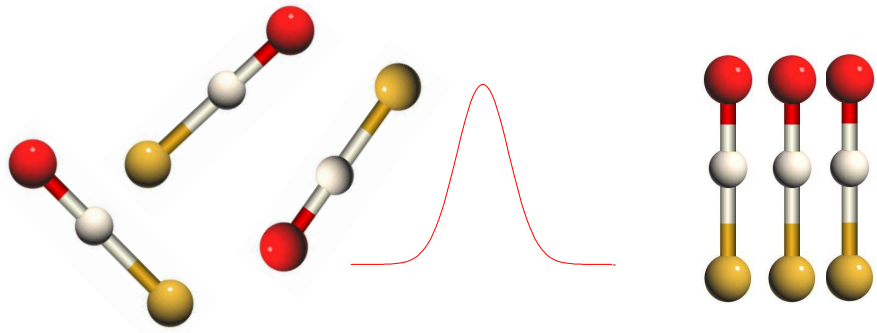

Figure 1.2: A half-cycle pulse orients an ensemble of molecules.

1.4 Triatomic hydrogen-bonded systems

Triatomic molecules, ABC, are common candidates for studying controlled unimolecular dissociation since they contain few atoms but several vibrational modes [9]. One particular class of triatomics, hydrogen-bonded bihalide anions XHY^-, has been extensively studied over the past thirty years, both theoretically [62, 63, 64, 65, 66, 67, 68, 69, 70, 71, 72] and experimentally, [73, 74, 75, 76, 77, 78, 79, 80, 81, 82, 83, 84, 85, 86]. One of the reasons the bihalide-hydrogen ions have received so much attention is the fact that the bond strengths are extraordinarily high in these systems. Whereas weak or "conventional" hydrogen bonds have a bond strength of 2.4 to 12 kcal/mol [87], the F–H bond strength in FHF^-, for example, was measured to be nearly 40 kcal/mol, with slightly decreasing bond strengths for the X–H bonds in $ClHCl^-$, $BrHBr^-$, and IHI^-, in that order [74, 75]. Another motivation for studying the bihalide ions is the ease at which the transition state $XHY^\ddagger$ can be probed via electron photodetachment, most notably demonstrated in the experiments of Neumark *et al.* [80, 81, 82, 83, 84]. In Neumark's experiments, a laser with fixed frequency ejects an electron from a stable linear anion, inducing a vertical transition to its neutral counterpart [80]. The resulting neutral species, XHY, is unstable and begins to dissociate. Along the reaction coordinate *perpendicular* to the dissociation coordinate, however, the transition-state complex continues to vibrate, thus giving rise to a structured photoelectron spectrum. The general scheme is the following:

$$XHY^- \xrightarrow{\hbar\omega} XHY^\ddagger + e^- \longrightarrow X + HY + e^- \;\; or \;\; XH + Y + e^-.$$

The kinetic energy of the ejected electrons, measured with about 10 meV (80 cm^{-1}) resolution, maps the topology of the ion's transition state, or the saddle point of the multi-dimensional PES [84]. Threshold photodetachment spectroscopy is closely related, but it has a much higher resolution of ~ 0.3 meV; in that method, electrons of nearly zero kinetic energy (ZEKE) are recorded as a function of laser frequency [88]. Recently, slow electron velocity-map imaging (SEVI) has been developed to record spectra over a

range of electron kinetic energies with less than 1 meV resolution [89]. In the present simulations, we will assume a (near-) ZEKE scenario, *i.e.* the transition from XHY^- to XHY + e^- proceeds without any significant electron kinetic energy. In this thesis, we study the vertical transition from anion to neutral species, but we will not treat the vibrational structure of transition states.

We have chosen two anions and their neutral counterparts to study, FHF^-/FHF and OHF^-/OHF. Whereas OHF^- has received relatively little attention, FHF^- has been the subject of many theoretical [62, 63, 65, 66, 69, 71, 90] and experimental [63, 65, 66, 67, 73, 74, 76, 77, 78, 91] investigations. Most of the research has been directed at characterizing the equilibrium geometry and the vibrational states of FHF^- in the gas phase, but discrepancies in the data exist, especially in the vibrational frequencies. More than thirty years ago, Almlöf performed some of the first *ab initio* calculations to determine an equilibrium F–F distance of 2.28 Å [62]. Using diode laser spectroscopy, Kawaguchi and Hirota measured an F–F internuclear distance of 2.278 Å, as well as the vibrational bands of FHF^-, ν_1(sym)=583 cm^{-1}, ν_2(bend)=1286 cm^{-1}, and ν_3(asym)=1331 cm^{-1} [77, 78]. Del Bene *et al.* investigated the vibrational anharmonicity of FHF^- and calculated an F–F bond distance of 2.282 Å and ν_1(sym) = 640 cm^{-1}, ν_2(bend)=1347 cm^{-1}, and ν_3(asym)=1244 cm^{-1}, at the CCSD(T)/aug′-cc-pVTZ level of theory [71]. Thorson *et al.* performed a comprehensive *ab initio* study of the vibrational dynamics of FHF^- and determined ν_1(sym) = 608 cm^{-1}, ν_2(bend) = 1363 cm^{-1}, and ν_3(asym) = 1565 cm^{-1} [63, 65, 66, 67]. The bond dissociation energy of FHF^- was measured by Illenberger *et al.* to be approximately 35 kcal/mol [76], and the bond energy of F–H was determined by Larson *et al.* to be nearly 40 kcal/mol [73, 74].

The radical anion OHF^- has been studied both theoretically [83, 92, 93, 94, 95, 96] and experimentally [83, 92], primarily to elucidate the energetics of the bi-molecular reaction of

$$OH(^2\Pi) + F(^2P) \rightarrow O(^3P) + HF(^1\Sigma^+)$$

which has an exothermicity of ∼1.5 eV [97]. In recent years, OHF^- has also gained some attention as an analog to the bihalide anions XHY^-. Specifically, the photoelectron spectrum has been studied to gain a better understanding of the energetics of the above reaction. Bradforth *et al.* measured photoelectron spectra [83], prompted by measurements of Sloan *et al.* who measured product-state distributions from the OH + F reaction [92]. The experimental photodetachment spectrum shows a maximum kinetic energy of 2.43 eV, an energy that can be assigned to the ground vibrational level of the products O + $HF_{v=0}$ [83]. Simulations also strongly indicate that a sequence of bands may be attributed to HF vibrational levels at resonances at low energies in the O + HF channel [93, 95]. Dixon *et al.* simulated the photodetachment spectrum of OHF^- using UMP4/6-31++G(d,p) *ab initio*

surfaces and calculated a branching ratio of $0.7 : 0.3$ for the product channels O + HF versus OH + F [93]. Most recently, González-Sánchez *et al.* performed multireference configuration interaction (MRCI) calculations to generate high quality 3D potential energy surfaces for the $^2\Pi$ ground state of OHF^- [95], and for the ground triplet ($^3\Pi$) state of OHF [94]. A photodetachment spectrum of OHF^- was calculated [95], as well as the transition state dynamics of OHF on several electronic surfaces [95, 96]. These results point to the absence of a barrier to the reaction $OH(^2\Pi) + F(^2P) \rightarrow O(^3P) + HF(^1\Sigma^+)$, in contrast to the results obtained by earlier investigations of Sloan *et al.* [92]. Therefore, although some of the existing data are inconclusive, all studies suggest the exoergicity of the reaction $OH(^2\Pi) + F(^2P) \rightarrow O(^3P) + HF(^1\Sigma^+)$. Unfortunately, to our knowledge, no experimental data on vibrational (IR) absorption spectroscopy of OHF^- is available for comparison.

1.5 Goals of this thesis

In Sections 1.1-1.3, a brief review of the field of laser-controlled reaction dynamics was presented, focusing on IR-laser mediated photodissociation. The two triatomic systems that we will study, FHF^- and OHF−, were reviewed in Section 1.4. In this section, we formulate the goals of this thesis and the topics that will be treated in the upcoming chapters.

A question that is central to reaction dynamics and which we will address in this thesis is the following: can laser radiation be used to control the unimolecular dissociation of a triatomic hydrogen-bonded molecule? To investigate this problem with our model systems FHF^- and OHF^-, we apply the mechanism suggested by Henriksen [31, 32], namely of few-cycle IR + UV laser pulse-mediated bond-selective dissociation.

In the first model system, FHF^-, the chemical products are equivalent and indistinguishable. In this case, our goal is to break the symmetry of the system and achieve significant wave packet displacement using a few-cycle IR pulse. Next, with an ultrashort UV pulse, we will excite the wave packet to a bond-selective region of the neutral PES and analyze the branching ratio of dissociation products. Isotope effects will also be studied for the heavier isotopomer FDF^-, in which IR and UV laser pulses will be re-optimized to achieve similar symmetry breaking in FDF^-. For these quantum dynamical simulations, FHF^- and FDF^- are assumed to be aligned in the direction of the electric field. As discussed in Section 1.3, the relative orientation of the reactants in the laser field is a non-trivial issue and limits the effectiveness of the proposed laser control scheme. The spatial separation of dissociation products F + HF will therefore be

analyzed for various initial molecular orientations of the anion FHF^-.

In the next system, OHF^-, the control of orientation will be treated explicitly using a HCP to give the molecule a "kick" of angular momentum in the direction of the field polarization. Resulting rotational wave packets will be analyzed to assess the degree of molecular orientation. Next, bond-selective dissociation will be investigated for pre-oriented OHF^-. The molecule has two distinct chemical products, $OHF^- \rightarrow O + HF$ or OH + F, so we seek to control the product branching ratio of the oriented molecule using few-cycle IR + UV laser pulses that are optimized for each dissociation channel.

For the simulated laser-driven dissociation reactions, wave functions and potential energy and dipole surfaces are required. For the surfaces, we will construct two-dimensional (2D) *ab initio* PESs for the anion/neutral pair, and permament dipole surfaces for the anions. From the potential energy surfaces, we can then calculate anharmonic equilibrium bond distances, as well as 2D anharmonic vibrational wave functions and eigenenergies for FHF^- and OHF^-, as well as for the corresponding heavier isotopomers, FDF^- and ODF^-. Anharmonic vibrational frequencies will be compared with harmonic values. Vibrational (IR) absorption spectra will also be calculated for FHF^- and FDF^-, as well as for OHF^- and ODF^-. Peak locations and relative intensities will be analyzed and compared with available experimental data. FHF^- and FDF^-, as well as for OHF^- and ODF^-. Peak locations and relative intensities will be analyzed and compared with available experimental data.

Finally, wave packet simulations will be carried out on the 2D PESs of the anion and neutral systems. Time-dependent wave packets will be obtained as solutions to the time-dependent Schrödinger equation, and numerical propagation of wave packets will be carried out on evenly spaced discretized grids, in discretized time steps.

1.6 Structure of thesis

The remainder of this thesis will consist of the following. In Chapter 2, fundamental quantum mechanical principles will be reviewed, beginning with the time-independent Schrödinger equation and the Born-Oppenheimer (B-O) approximation. Within the B-O approximation, solutions to the electronic and nuclear Schrödinger equation will be presented. Next, the time-dependent Schrödinger equation will be discussed, along with the interaction of matter with an electromagnetic field. Chapter 2 will end with an in-depth review of angular momentum and the rigid rotor model, in the context of molecular

orientation. Chapter 3 presents the results of the 2D quantum chemical calculations for FHF^- and OHF^-, including PESs for the anion and neutral species, permanent dipole surfaces for the anions, and anharmonic vibrational wave functions of the anionic species. Isotope effects will also be discussed in this context. Vibrational (IR) absorption spectra for FHF^- and OHF^- will also be presented in Chapter 3. Chapter 4 will contain all results of quantum dynamical simulations for FHF^-/FHF and OHF^-/OHF. Results for the selective bond-breaking of *pre-oriented* FHF^- will be presented first, followed by a discussion of dissociation yields for various molecular orientations. Results for OHF^- focus first on an active control pulse to orient the anion in the laser field, followed by the results of bond-selective dissociation. Finally, we consider possible sources of error that may have affected the results of quantum dynamical calculations. Chapter 5 will summarize the work presented in this thesis and will make some brief remarks about ongoing and future work.